Clays and Clay Minerals, Vol. 58, No. 1, 72–78, 2010.

STRUCTURE AND PROPERTIES OF HYDROGENATED NITRILE RUBBER/ORGANO-MONTMORILLONITE NANOCOMPOSITES

ZHENG GU[1,2], GUOJUN SONG[2], WEISHENG LIU[1,*], SHUJING YANG[2], AND JIANMING GAO[2,3]

[1] Department of Chemistry and State Key Laboratory of Applied Organic Chemistry, College of Chemistry and Chemical Engineering, Lanzhou University, Lanzhou 730000, China
[2] Institute of Polymer Materials, Qingdao University, Qingdao 266071, China
[3] Qingdao TKS Sealing Industry Company, Qingdao 266071, China

Abstract—The aim of the work was to study the effect of organo-montmorillonite (OMt) on the properties of hydrogenated nitrile rubber (HNBR)/OMt nanocomposites. The nanocomposites were prepared by a melt intercalation method. The structure of the composites was studied by transmission electron microscopy (TEM) and X-ray diffraction (XRD). The behavior of stress-strain, aging resistance, solvent resistance, and the dynamic mechanical properties of HNBR/OMt nanocomposites were investigated. The TEM and XRD results showed that the OMt layers were dispersed homogeneously in the HNBR matrix. The HNBR/OMt nanocomposites showed excellent mechanical properties which were attributed to the nanometer scale dispersion and strong interaction between the HNBR and OMt. The composites possessed excellent aging resistance and oil resistance, which improved with OMt content. Dynamic mechanical analysis showed that the glass-transition temperature, T_g, of the HNBR/OMt nanocomposites was increased and the nanocomposites had a good rolling resistance in comparison to pure HNBR. The composites displayed better dynamic mechanical properties.

Key Words—Dynamic Mechanical Properties, HNBR, Hydrogenated Nitrile Rubber, Organo-montmorillonite, OMt, Nanocomposites, Mechanical Properties, Oil Resistance.

INTRODUCTION

Clay/polymer nanocomposites are of great interest both scientifically and in terms of industrial applications (Kojima *et al.*, 1993; Messersmith and Giannelis, 1995; Giannelis, 1996; Ray and Okamoto, 2003). Compared to their micro- or macro-composites, the nanocomposite version exhibits excellent properties because of the fine phase dimension and special phase structure involved. In general, polymer/clay nanocomposites with a relatively small loading of filler have superior mechanical properties, thermal stability, flame retardancy, and gas-barrier properties (Gao *et al.*, 2008; Karger-Kocsis and Wu, 2004). The improvements in the properties are the result of the nm-scale dispersion of the clay in the polymer matrix. The polymer/clay nanocomposites are generally classified into three groups according to their structure: nanocomposites with intercalated, exfoliated, or both structures. Completely exfoliated nanocomposites are desirable because the exfoliated layers exhibit the greatest reinforcement (Wu *et al.*, 2005; Utracki *et al.*, 2007; Sengupta *et al.*, 2007). The dispersion of layered silicates in rubber/organo-clay nanocomposites is a key parameter with respect to their reinforcement (Kong *et al.*, 2008). Superior nanocomposites originate not only from the strong interactions between the elastomer and the clay but also from the good dispersion of clay layers in the rubber matrix. The dispersion state of the clay in nanocomposites is determined by factors such as matrix properties, clay nature, strength of interaction, rubber recipe, and compounding as well as curing conditions (Wang *et al.*, 2008).

The HNBR, while having high performance characteristics, is an expensive material, which has led to the investigation of blends with other elastomers (Severe and White, 2000). Generally, HNBR is immiscible with most commercial elastomers but is, however, miscible with certain chlorinated polyethylenes and polyvinyl chloride. Gatos *et al.* (2005) studied the effect of peroxide vulcanization on organo-clay dispersion in HNBR/OMt nanocomposites. The morphologies and dynamic mechanical properties of hydrogenated acrylonitrile butadiene rubber filled with organophilic layered silicates were investigated by Herrmann *et al.* (2006). Wang *et al.* (2008) studied the effect of temperature, pressure, and treatment time on the microstructural changes in HNBR/OCN (organophilic clay nanocomposite) compounds. The present study focused on explaining the structure-properties relations and aimed to develop an HNBR/clay nanocomposite with good mechanical properties and oil resistance using organo-modified montmorillonite (OMt). The HNBR/OMt nanocomposites were prepared by a melt-mixing process and were characterized by XRD and TEM. The effects of clay on the mechanical properties, thermal stability, and solvent-resistance properties of HNBR were also studied.

* E-mail address of corresponding author:
Liuws@lzu.edu.cn
DOI: 10.1346/CCMN.2010.0580107

EXPERIMENTAL

Materials

The montmorillonite was obtained from a clay mine in Shandong Province, China; its cation exchange capacity (CEC) is 119 meq/100 g. The dimethyl ditallow ammonium-modified montmorillonite (OMt) was produced by the Institute of Polymer Materials in Qingdao University, China. The HNBR (Therban C3406) was provided by Lanxess (Leverkusen, Germany) and has a Mooney viscosity ML (1+4) 100ºC = 63. The other materials used were commercial products (and of AR grade).

Preparation of HNBR/OMt nanocomposites

The HNBR/OMt nanocomposites were prepared in an open, two-roll mill. The OMt was mixed with the elastomer first. The vulcanizing agents were then added at the end of the mixing. The amounts of OMt added to HNBR were 0, 3, 6, 9, 12, and 15 wt.% of OMt to rubber. The recipes for the HNBR/OMt compounds are listed in Table 1. The specimens were first cured at 170ºC in an electrically heated hydraulic press for 10 min.

Measurement

Transmission electron microscopy. Observation by TEM was performed on ultra-thin films prepared by cryo-ultramicrotomy using a JEM-1200EX (JOEL, Japan) at an acceleration voltage of 80 kV.

X-ray diffraction. To establish the interlayer spacing of Na-Mt, of organo-modified clay, and of their composites, XRD scattering patterns between 2 and 10º were obtained using an X-ray diffractometer (Rigaku 2500PC, Japan) with operating conditions of 40 kV, 200 mA, and CuKα radiation (having a wavelength of 0.154 nm at room temperature).

Mechanical properties. Tensile tests were carried out on 2 mm thick dumbbells (type: S1 according to DIN 53504) on a DXLL-50000 material tester (Dirs Company, China) at a crosshead speed of 500 mm/min and room temperature. From the related stress-strain curves, other than the final properties, the stress values at 300% elongations were also read (ISO 37).

Table 1. Recipe for the HNBR/OMt compounds.

Material	Parts
HNBR (Therban C3406)	100
OMt	Various
SA (stearic acid)	0.5
ZnO_2 (zinc peroxide)	8
TT (trioctyl trimellitate)	1
TETD (tetramethyl thiuram disulfide)	1.5
CZ (cyclohexyl-2-benzothiazole sulfenamide)	1.5
S (sulfur)	0.5

Thermo-gravimetric analysis. Thermo-gravimetric analysis (TGA) of the samples was performed using a thermo-gravimetric analyzer (TGA/STDA851, Mettler Toledo, Shanghai, China) attached to an automatic programmer, from ambient temperature to 600ºC at a programmed heating rate of 10ºC/min in an air atmosphere. A sample weight of ~15 mg was used for the measurements.

Dynamic mechanical thermal analysis. The dynamic mechanical properties of the nanocomposites were measured using a dynamic mechanical thermal analyzer (DMTA V, Rheometrics Science Corp., Piscataway, New Jersey, USA) at a fixed frequency of 1 Hz with 3ºC/min heating rate using liquid nitrogen for the sub-ambient region. Loss factors (tanδ) were obtained by rectangular tension mode and the strain amplitude over the temperature range −80 to 50ºC. The dimensions of the specimens used were 20 mm long × 10 mm wide × 2 mm thick.

Oil-resistance properties. Swelling studies were performed as per the ASTMD 471-98 test method. Rectangular test specimens measuring ~25 mm × 50 mm were cut from the molded layers, weighed accurately, and immersed in ASTM #3 oil at 150ºC for 70 h. The volume swell was calculated as

$$\text{Volume swell} \quad (\%) = \frac{M_3 - M_4}{d(M_1 - M_2)} \times 100$$

where M_1 and M_2 are the specimen weights in air and water, respectively, before immersion, M_3 and M_4 are the specimen weights in air and water, respectively, after immersion, and d is the density of the immersion liquid.

Air aging tests. Aging studies were carried out in an air-circulated aging oven at 200ºC for 70 h. The samples were kept at room temperature for 24 h after aging and the tensile properties were measured as described above.

RESULTS AND DISCUSSION

Morphology and structure of HNBR/OMt nanocomposites

X-ray diffraction and TEM are complimentary techniques used to characterize the structure of the nanocomposites. The TEM allows a qualitative understanding of the structure of the nanocomposites through direct observation, and has been used to estimate quantitatively the distance between the clay layers (*e.g.* Galimberti *et al.*, 2008). On the other hand, XRD is used to determine the interlayer spacing of clay layers in the

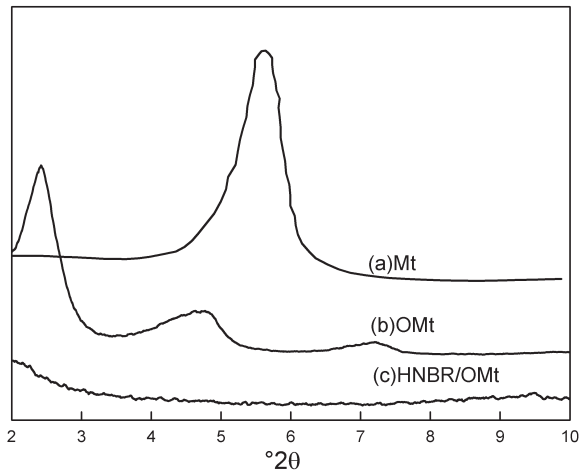

Figure 1. XRD patterns of Mt, OMt, and HNBR/OMt (3 wt.%)

original clay and in the polymer/clay nanocomposites. The XRD pattern of Mt, OMt, and HNBR/OMt nanocomposite (3 wt.%) (Figure 1) revealed that the original Mt showed a 001 reflection at 5.57º2θ, corresponding to a basal spacing of 1.58 nm. After organic modification using ammonium, the OMt showed a 001 reflection at 2.41º2θ, corresponding to a larger basal spacing of 3.66 nm, and indicating the intercalation of ammonium within the Mt layers. Such intercalation is desirable for making intercalated and exfoliated polymer/clay hybrids. When intercalation of rubber macromolecules into the interlayer occurs, the XRD peak will shift to a smaller angle for the intercalated nanocomposites, and if the silicate layers are exfoliated completely, no diffraction peaks will be observed because of the disorder of the layers or the larger interlayer space, beyond the resolution of XRD (Wang *et al.*, 2005). The 001 reflection of nanocomposites with 3 wt.% OMt disappeared over the range 2−10º. The XRD patterns of the HNBR/OMt nanocomposites showed no reflections in the 2−10º2θ range, indicating the loss of any order in the direction perpendicular to the structural layers and, as a consequence, suggesting exfoliation of the OMt.

X-ray diffraction may not reveal the real microstructures due to problems such as weak diffraction intensity and poor peak resolution for those nanocomposites with small clay content and because of the overlapping diffraction patterns of the exfoliated structure and the intercalated structure (Galgali *et al.*, 2001). Transmission electron microscopy images of HNBR/OMt nanocomposites (Figure 2) contained dark lines and areas representing OMt layers and aggregates, and light

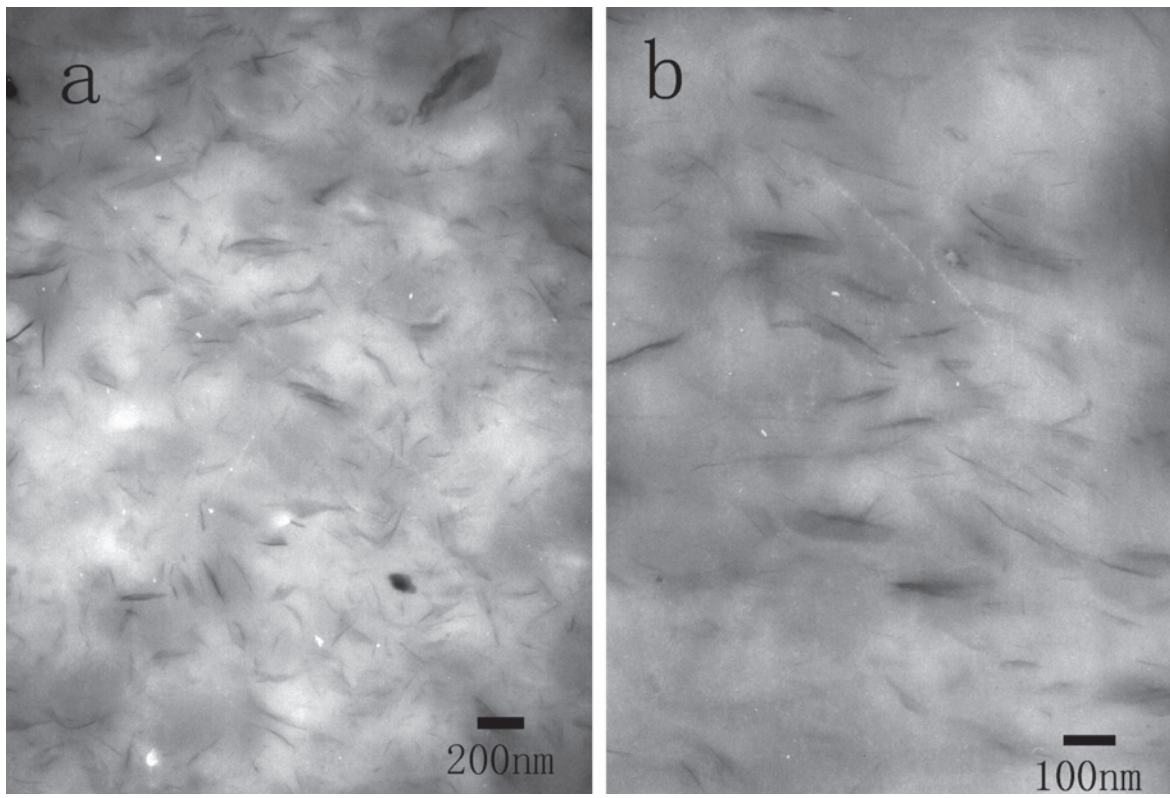

Figure 2. TEM images of HNBR/OMt nanocomposites with 3 wt.% OMt: (a) 200 nm; (b) 100 nm.

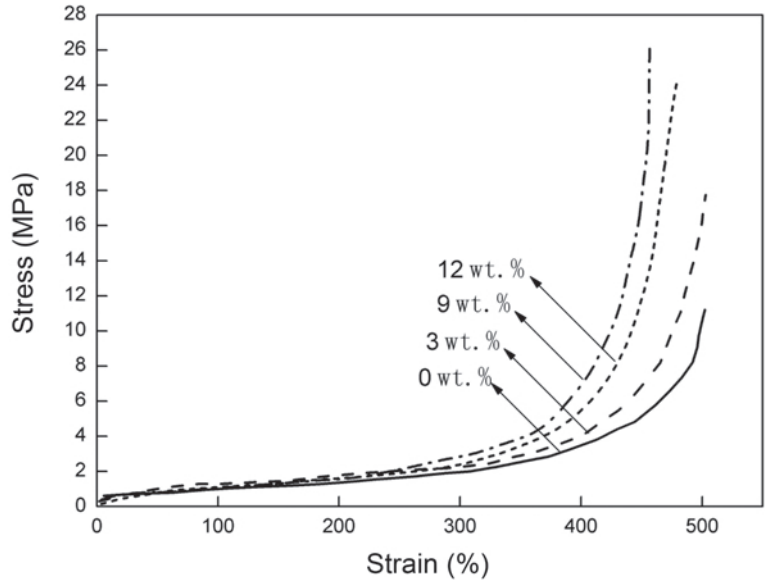

Figure 3. Stress-strain curves of HNBR/OMt nanocomposites with different OMt contents.

areas for the rubber matrix. The thickness of most of the clay-layer bundles was in the range 30−40 nm and ~100−300 nm long. Low-magnification TEM images clearly show clay layers which were well dispersed in the HNBR matrix. High-magnification TEM images revealed some single, exfoliated clay layers in the HNBR matrix. The TEM images also show an homogeneous distribution of particles as well as isolated layers in the HNBR matrix.

Mechanical properties of HNBR/OMt nanocomposites

The stress-strain curves of HNBR/OMt nanocomposites with different OMt contents (Figure 3) show that, with increase in the OMt content up to 9 wt.%, the tensile modulus and tensile strength increased. The results may be due to the strong interactions between the OMt layer and rubber chains associated with larger contact surface area, leading to greater restraint on the motion of the rubber chains. When the OMt content was 12 wt.%, however, the mechanical properties decreased, which was considered to be due to the formation of OMt aggregates (Gao *et al.*, 2008).

The mechanical properties of HNBR/OMt nanocomposites also changed as a function of OMt content (Table 2). The tensile strength and tear strength of HNBR/OMt nanocomposites increased with OMt content up to 9 wt.%. Compared to the pure HNBR, with the increase in OMt content the modulus at 300% of HNBR/OMt nanocomposites was enhanced, while the elongation at break decreased. The decrease in elongation at break can be attributed to the stress-induced crystallization behavior. The improvement in the mechanical properties could be attributed to two reasons: (1) nano-dispersed OMt with high aspect ratio possesses a greater stress-bearing capability and efficiency; and (2) stronger interactions between OMt clay and rubber chains associated with larger contact surface area result in greater restraint on the motion of rubber chains (Kojima *et al.*, 1993). Further addition of OMt led to a decrease in mechanical properties. As the OMt content increased, some OMt layers began to aggregate (Shi and Gan, 2008) and the introduction of yet further OMt layers impeded the stress-induced crystallization of HNBR (Wang *et al.*, 2005). The formation of OMt aggregates reduced the interfacial area between polymer and OMt layers, leading to decreases in the mechanical properties.

Thermal properties of HNBR/OMt nanocomposites

Nanolayered silicates display good barrier behavior, which can improve the thermal stability of nanocomposites. The alkyl ammonium cations in the OMt could suffer decomposition following the Hofmann elimination reaction (Liang *et al.*, 2003). Degradation of OMt might catalyze the degradation of polymer matrices,

Table 2. Mechanical properties of HNBR/OMt with different OMt contents.

OMt content (wt.%)	Modulus at 300% (MPa)	Tensile strength (MPa)	Elongation at break (%)
0	1.88	12.41	501
3	2.37	18.24	497
6	2.32	22.64	483
9	2.72	25.77	478
12	2.94	23.75	456

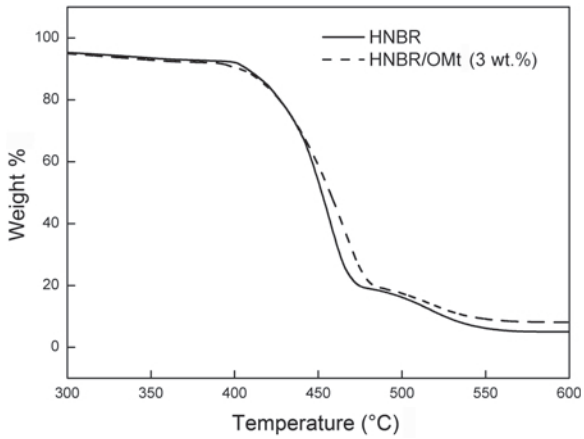

Figure 4. TGA curves of HNBR and HNBR/OMt nanocomposites (3 wt.%).

which could reduce the thermal stability.

The thermal stability of HNBR and HNBR/OMt nanocomposites were tested by TGA and differential thermogravimetry (DTG) in air atmosphere (Figures 4 and 5). At the initial stage of degradation (before 410ºC), due to the Hofmann elimination reaction and the clay-catalyzed degradation, the HNBR/OMt nanocomposites degraded faster than pure HNBR. When the temperature was >410ºC, HNBR/OMt nanocomposites were more stable than pure HNBR. The onset temperature and the decomposition temperature of HNBR/OMt composites were greater than those of pure HNBR.

The DTG curves (Figure 5) showed that the maximum decomposition temperature (T_{max}) was obtained, which increased from 457ºC (pure HNBR) to 467ºC (HNBR/OMt (3 wt.%)). When the OMt layers were well dispersed, the layer structure exhibited much resistance to thermal degradation, thereby hindering the evaporation of small molecules generated in the thermal decomposition and limiting the continuous decomposition of the HNBR matrix. Compared with the Hofmann elimination reaction and its catalysis degradation, the gas-barrier behavior dominated the thermal properties of HNBR/OMt nanocomposites above 410ºC. Above 410ºC, Hofmann elimination reaction and its catalytic degradation affected the thermal properties of the composites slightly with increasing temperature, resulting in the improvement of the thermal stability of the nanocomposites.

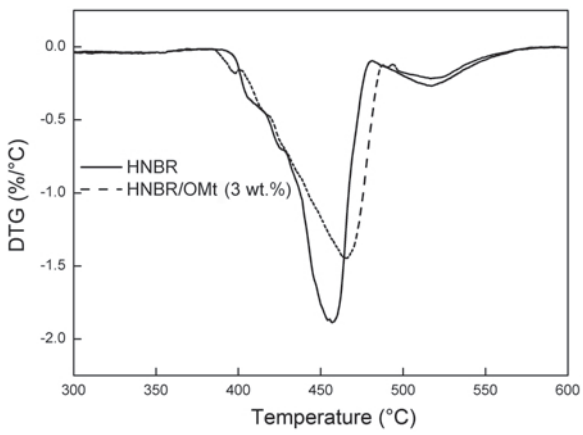

Figure 5. DTG curves of HNBR and HNBR/OMt nanocomposites (3 wt.%).

Heat and oil resistance of HNBR/OMt nanocomposites

The results of tensile-strength testing before and after air aging at 200ºC for 70 h and aging in ASTM #1 oil at 150ºC for 70 h were compared (Table 3). The oil-resistance measurements of HNBR/OMt nanocomposites (Figure 5) showed the volume-swell values in ASTM #1 oil at 150ºC for 70 h. The tensile strength increased initially and then decreased with increased OMt content after aging. The volume swell decreased gradually with increase in OMt content, indicating the increased probability of formation of three-dimensional network structures which resist the penetration of oil into the nanocomposites (Figure 6), caused by good dispersion of OMt and the strong interactions between OMt and the polymer matrix. The presence of nano-dispersed impermeable OMt layers with excellent barrier properties decreased the chemical transport rate by lengthening the average diffusion path in the polymer matrix (Gatos *et al.*, 2005).

Dynamic mechanical properties of HNBR/OMt nanocomposites

The loss factor (tanδ) of pure HNBR and the HNBR/OMt nanocomposites *vs.* temperature (Figure 7) can be used to measure dynamic mechanical properties and to examine the degree of filler-matrix interaction of HNBR/OMt nanocomposites. The glass transition temperature (T_g) of pure HNBR was −18.88ºC, and increased to −15.53ºC for the HNBR/OMt nanocomposite with 3 wt.% OMt. The HNBR/OMT nanocomposites showed a greater glass transition temperature, smaller tanδ peak value, and slightly broader glass transition region than pure HNBR.

Table 3. Tensile strength (MPa) of HNBR/OMt nanocomposites after heat aging and oil aging.

OMt content (wt.%)	Unaged samples	Heat aging at 200ºC for 70 h	Oil aging at 150ºC for 70 h (ASTM #1 oil)
0	12.41	9.84	9.70
3	18.24	15.07	15.37
6	22.64	19.17	19.77
9	25.77	22.56	22.85
12	23.74	19.68	19.88

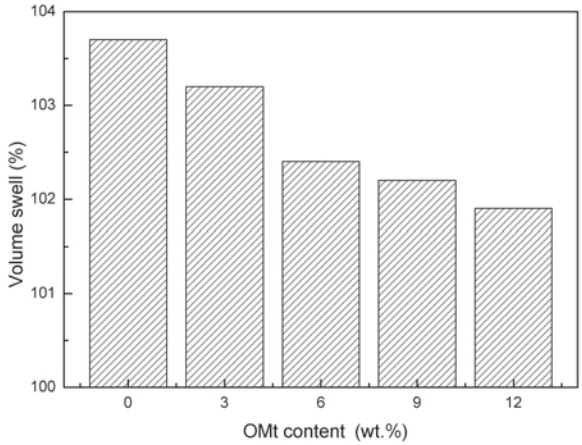

Figure 6. Volume swell of HNBR/OMt nanocomposites with different OMt contents.

Those nanocomposites also had a stronger filler network and larger interfacial hysteresis confinement of rubber molecules by OMt. All should be attributed to the decreased mobility of rubber molecules caused by the OMt layers. At 0ºC, the HNBR/OMt nanocomposite had a greater tanδ value than pure HNBR, while its tanδ was less than that of pure HNBR at 50ºC, indicating that the nanocomposite had a good roll resistance.

CONCLUSIONS

The HNBR/OMt nanocomposites were prepared by melt intercalation. Analysis by TEM and XRD indicated that the OMt layers were exfoliated homogeneously in the HNBR matrix. The HNBR/OMt nanocomposites exhibited excellent mechanical properties, thermal stability, and oil resistance. Compared to the pure HNBR, the nanocomposites exhibited a greater glass-transition temperature and smaller tanδ peak value, indicating that the nanocomposites had a good rolling resistance.

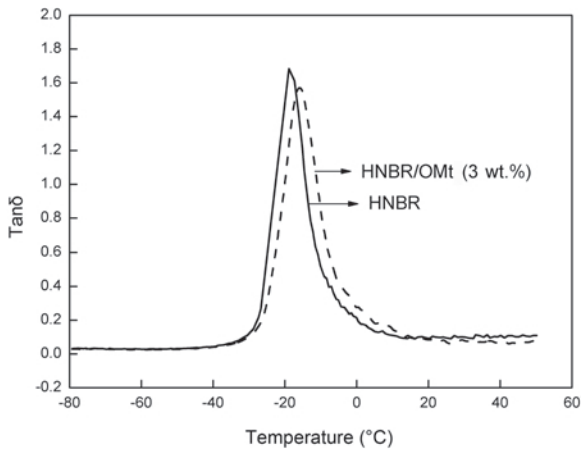

Figure 7. Curves of tanδ *vs.* temperature for pure HNBR and HNBR/OMt nanocomposites (3 wt.%).

ACKNOWLEDGMENTS

The authors thank the TEM and XRD staff for helping with sample testing for this study. They also thank the reviewers for critical comments which improved this manuscript.

REFERENCES

Galgali, G., Ramesh, C., and Lele, A. (2001) A rheological study on the kinetics of hybrid formation in polypropylene nanocomposites. *Macromolecules*, **34**, 852−858.

Galimberti, M., Senatore, S., Conzatti, L., Costa, G., Giuliano, G., and Guerra, G. (2008) Formation of clay intercalates with organic bilayers in hydrocarbon polymers. *Polymer for Advance Technologies*, **20**, 135−142.

Gao, J.M., Gu, Z., Song, G., Li, P., and Liu, W. (2008) Preparation and properties of organo-montmorillonite/fluoroelastomer nanocomposites. *Applied Clay Science*, **42**, 272−275.

Gatos, K.G., Százdi, L., Pukánsky, B., and Karger-Kocsis, J. (2005) Controlling the deintercalation in hydrogenated nitrile rubber (HNBR)/organo-montmorillonite nanocomposites by curing with peroxide. *Macromolecular Rapid Communication*, **26**, 915−919.

Giannelis, E.P. (1996) Polymer layered silicate nanocomposites. *Advanced Materials*, **8**, 29−35.

Herrmann, W., Uhl, C., Heinrich, G., and Jehnichen, D. (2006) Analysis of HNBR-montmorillonite nanocomposites: morphology, orientation and macroscopic properties. *Polymer Bulletin*, **57**, 395−405.

Karger-Kocsis, J. and Wu, C.M. (2004) Thermoset rubber/layered silicate nanocomposites. Status and future trends. *Polymer Engineering and Science*, **44**, 1083−1093.

Kojima, Y., Usuki, A., Kawasumi, M., Okada, A., Kurauchi, T., and Kamigaito, O. (1993) Sorption of water in nylon 6-clay hybrid. *Journal of Applied Polymer Science*, **49**, 1259−1264.

Kong, Q.H., Ruibin, Lv., and Zhang, S. (2008) Flame retardant and the degradation mechanism of high impact polystyrene/Fe-montmorillonite nanocomposites. *Journal of Polymer Research*, **15**, 453−458

Liang Z.M., Yin, J., and Xu, H.-J. (2003) Polyimide/montmorillonite nanocomposites based on thermally stable, rigid-rod aromatic amine modifiers. *Polymer*, **44**, 1391−1399.

Messersmith P.B. and Giannelis E.P. (1995) Synthesis and barrier properties of poly(-caprolactone)-layered silicate nanocomposites. *Journal of Polymer Science Part A: Polymer Chemistry*, **33**, 1047−1057.

Ray, S.S. and Okamoto, M. (2003) Polymer/layered silicate nanocomposites: a review from preparation to processing. *Progress Polymer Science*, **28**, 1539−1641.

Sengupta, R., Chakraborty, S., Bandyopadhyay, S., Dasgupta, S., Mukhopadyhyay, R., Auddy, K., and Deuri, A.S. (2007) A short review on rubber/clay nanocomposites with emphasis on mechanical properties. *Polymer Engineering and Science*, **47**, 1956−1974.

Severe, G. and White, J.L. (2000) Physical properties and blend miscibility of hydrogenated acrylonitrile-butadiene rubber. *Journal of Applied Polymer Science*, **78**, 1521−1529.

Shi, X.D. and Gan, Z.H. (2008) Preparation and characterization of poly(propylene carbonate)/montmorillonite nanocomposites by solution intercalation. *European Polymer Journal*, **43**, 4852−4858.

Utracki, L.A., Sepehr, M., and Boccaleri, E. (2007) Synthetic, layered nanoparticles for polymeric nanocomposites (PNCs). *Polymer for Advance Technologies*, **18**, 1−37.

Wang, Y.Q., Zhang, H., Wu, Y., Yang, J., and Zhang, L. (2005) Preparation and properties of natural rubber/rectorite Nanocomposites. *European Polymer Journal*, **41**, 2776–2783.

Wang, X.P., Huang, A.-M., Jia, D.-M., and Li, Y.-M. (2008) From exfoliation to intercalation – changes in morphology of HNBR/organoclay nanocomposites. *European Polymer Journal*, **44**, 2784–2789.

Wu, Y.P., Wang, Y.-Q., Zhang, H.-F., Wang, Y.-Z., Yu, D.-S., Zhang, L.-Q., and Yang, J. (2005) Rubber – pristine clay nanocomposites prepared by co-coagulating rubber latex and clay aqueous suspension. *Composites and Science Technology*, **65**, 1195–1202.

(*Received 17 February 2009; revised 2 September 2009; Ms. 284; A.E. F. Bergaya*)